

Ultrasound-assisted removal of brilliant green from aqueous solution using banana and jackfruit peels

Pranav D Pathak¹, Paradeep Singh² & Sachin A Mandavgane*¹

¹Department of Chemical Engineering Visvesvaraya National Institute of Technology, Nagpur 440 010 India

²Department of Biotechnology, Lovely professional university, Chandigarh, Punjab, India.

Email: sam@che.vnit.ac.in

Received 7 November 2016; accepted 27 April 2017

The potential use of banana (BP) and jackfruit peel (JFP) as eco-friendly and low-cost adsorbents for removal of brilliant green (BG) dye from waste water in the presence of ultrasonic field has been studied. Batch process has been used for adsorption kinetic, equilibrium, and thermodynamic studies. Results show that the amount of BG adsorbed and the rate of adsorption increased in presence of ultrasonic field. The adsorption of BG onto BP and JFP is fast (equilibrium time for the adsorption is about 25 min) and follows the pseudo-second-order kinetic model. The Langmuir isotherm shows the best fit for the adsorption of BG onto BP, where as both Langmuir and Freundlich adsorption isotherms show best fit for the adsorption of BG onto JFP ($R^2=0.99$). The maximum adsorption capacities calculated using the Langmuir isotherm are 21.74 and 31.25 mg/g at 313 K for BP and JFP, respectively. The ΔG values are negative at all operating temperatures, confirming that the adsorption of BG is spontaneous and thermodynamically favorable. The positive value of ΔS suggests the increased randomness at the adsorbate-adsorbent interface. Overall, our study suggests that BP and JFP can be used as an ecofriendly and low-cost agro-material for removal of BG dye from aqueous solutions.

Keywords: Banana peel, Jackfruit peel, Brilliant green, Adsorption, Ultrasonic

Increasing industrialization has led to increased pollution by discharging different types of toxic pollutants into water bodies. These toxic pollutants mainly include organic and inorganic materials such as aromatic compounds, heavy metals, dyes and pigments¹. The effluents discharged from textile, food, printing, tannery, pulp and paper industries contain dye as a primary component, which imparts abhorrent color to the effluent stream. The dye-containing water is environmentally and aesthetically not acceptable owing to its high chemical oxygen demand (COD) loading and strong persistent colour. Moreover, the synthetic dyes have great stability due to their aromatic structure and thus, they do not degrade very easily²⁻⁴. Many dyes are considered as toxic and produce mutagenic and carcinogenic effects, which significantly affect both human health and aquatic biota. Thus, there is a need to identify effective and efficient methods to remove these dyes from waste waters^{4,5}.

Brilliant green (BG) is a dye that belongs to the triphenylmethane group. It is widely used in paper printing, biological stain, textile dyeing, dermatological agent, and veterinary medicine. Like

most other synthetic dyes, BG produces mutagenic and carcinogenic effects, which affect the human health and cause irritation to the respiratory and gastrointestinal tracts. Besides, BG is reported to cause nausea/vomiting and diarrhea in humans and affects aquatic life. BG produces nitrogen, carbon, and sulfur oxides upon degradation. Thus, advanced technologies must be developed to remove BG from wastewater in order to protect the environment and human health from its adverse effects⁶⁻⁸.

Various methods such as coagulation/flocculation, biodegradation, adsorption, chemical oxidation, ozone treatment, membrane filtration, photocatalysis, electrochemical, and aerobic and anaerobic microbial degradation have been used for the treatment of dye-containing wastewaters. Among these methods adsorption is found to be attractive due to its high efficiency, effectiveness, simple design and operation, and low cost^{1,9,10}. Several studies have reported on utilization of natural adsorbents for adsorption of BG from wastewaters, including *Psidiumguajava* leaves, *Solanumtuberosum* peels⁴, neem leaves⁵, oxidized cactus fruit peel⁶, activated carbon prepared from acorn¹¹, acid-activated watermelon rind¹², spent tea

leaves, jackfruit peels, rambutan peels, and mangosteen peels¹³. Some studies have also reported on utilization of synthetic adsorbents such as RHS-MCM-41², poly(acrylic acid) hydrogel composite³, and surfactant doped polyaniline/MWCNTs composite⁷ for this purpose.

In the recent past, ultrasound has proven to be a very useful tool for the enhancement of adsorptive separation by intensifying the mass-transfer characteristics and breaking the affinity between adsorbent and adsorbate¹⁴. Ultrasound waves are mechanical waves, produced by variation of density and pressure, with above human hearing threshold (~18 kHz) frequencies¹⁵. The process of adsorption mainly takes place by a mass-transfer reaction between an adsorbent and an adsorbate and is controlled by diffusion-convection in the system. The overall mass-transfer resistance can be reduced by making the system more turbulent (i.e., by increasing the convection in the medium). Ultrasound and its secondary effects, such as cavitation, nucleation, growth, and transient collapse of tiny gas bubbles due to the propagation of a pressure wave through a liquid, can create turbulence in the medium, which improves the mass-transfer characteristics. This improvement in the system can be attributed to physical phenomena such as microturbulence, microstreaming, acoustic (or shock) waves, and microjets. The shock waves produced have the potential to create turbulence at the microscopic level in the interfacial films surrounding the solid particles. Production of acoustic waves by sound wave is due to the movement of the medium. In other words, this is the conversion of sound to kinetic energy. The ultrasonic field does not alter the equilibrium characteristics of the adsorption system, and only enhances the rate of mass transfer in the concentration gradient direction, similar to that of acatalytic action¹⁶⁻¹⁹. There is an increasing use of ultrasonic waves for removal of dyes from wastewater in recent times²⁰⁻²².

This study investigates the use of banana peel (BP) and jackfruit peel (JFP) for the removal of BG from aqueous solutions by utilizing high-frequency ultrasound waves. Both BP and JFP are extensively used adsorbents for the removal of cationic dyes from wastewater¹. To standardize this system, first the physicochemical characterization of BP and JFP is carried out, and then the effect of adsorbent dose, time, initial concentration, and temperature

on adsorption of BG is analyzed. In addition, kinetic, equilibrium, and thermodynamic studies were conducted in batch process.

Experimental Section

Material and its preparation

The two adsorbents (i.e., BP and JFP) were prepared as reported earlier²³. BP and JFP were collected from a local fruit market in Nagpur (Maharashtra, India). The adsorbents were initially washed several times with tap water, and then with double-distilled water to remove any physical impurity on the surface. They were then cut into small pieces and dried under sunlight until achieving constant weight. Finally, the samples were crushed and passed through 0.15-0.71 mm sieves. Before use, both BP and JFP were stored in sealed bags, which were kept inside desiccators to avoid contact of moisture from humidity.

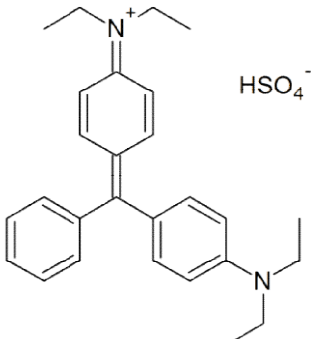
Chemicals

A stock solution of 1000 mg/L was prepared by dissolving 1 g of BG (Merck, India) in 1 L of deionized water. This stock solution was then used to prepare solutions of different concentrations as required for experiments. The pH of the solution was adjusted by adding 0.1N of NaOH/HCl (Fisher Scientific, USA). Fresh dilutions were made for each experiment and in all experiments only analytical-grade chemicals were used. The physical properties and chemical structure of BG are presented in Table 1.

Experimental setup

An ultrasound bath (PCI Analytics model: 1.5L50H, India; capacity 1.5 L) operating at a

Table 1 — Properties and characteristics of BG.

Generic name	Brilliant green
Chemical formula	C ₂₇ H ₃₃ N ₂ .HO ₄ S
Molecular weight (g/mol)	482.64
Solubility in water g/100 mL	100 g/L at 20°C
λ_{\max} (nm)	624
Chemical structure	

frequency of 36 ± 3 kHz with a 50-W power was used for sonication of the adsorption mixture. For each experimental run, two-thirds of the ultrasonic bath was filled with water at a desired temperature (30°C , 40°C , or 50°C), which would dip the flask in the water to about 75% of its height. Because the intensity of ultrasonic field changes based on the position of the flask in the bath, which subsequently affects the generation of results, the flask was placed at the center of the bath in each experiment using a burette stand with a clamp attached to it. The water in the bath was changed every after 10 min to avoid the substantial rise in temperature during the experiment. The average temperature of water in the bath was maintained in the range less than ($\pm 2^\circ\text{C}$)¹⁶. A thermometer was used for temperature monitoring.

Batch adsorption studies

Batch adsorption studies were performed to evaluate the effect of different parameters such as adsorbent dosage, contact time, initial BG concentration, and temperature. Batch adsorption studies were carried out in stoppered 150-mL Erlenmeyer flasks. A stock solution of BG (1000 mg/L) was prepared by dissolving 1 g of dye in deionized water, and other required concentrations (20-150 mg/L) were prepared by subsequent dilution of this stock solution. The standard batch adsorption procedure explained in the "Experimental Setup" section was followed. In each flask, 50 mL of dye solution was mixed with a predefined amount of adsorbent. After each experimental run, the solutions were filtered and the dye concentration of the filtrate was measured by a spectrophotometric method using a UV-1800 spectrophotometer at 624 nm (Shimadzu, Japan). Experiments were executed in triplicate, and average values are reported.

The percentage of adsorption and adsorption capacity q_e (mg/g) of the two adsorbents at equilibrium were calculated using the following equations:

$$\% \text{ adsorption} = \frac{(C_0 - C_e)}{C_0} \times 100 \quad \dots (1)$$

$$q_e = \frac{(C_0 - C_e)V}{w} \quad \dots (2)$$

Finally, the equilibrium data obtained were applied to various kinetic, isotherm, and thermodynamic models to define the best appropriate model.

Instrumentation and characterization

Proximate analysis of adsorbents was carried out according to the standard procedure for coal²⁴. The ultimate analysis was carried out using the Elementer, Vario Micro cube model. The BET surface area of adsorbents was calculated using Smart Sorb 92/93 surface area analyzer. The elemental analysis (XRF) of BP and JFP was carried out using an elemental analyzer (PAN analytical, model: PW2403). Scanning electron microscopic (SEM) images of adsorbents were captured using a scanning electron microscope (JSM 7600F). FTIR spectra of adsorbents and dye-loaded adsorbents were obtained using the KBr disk method (Thermo Scientific, Nicolet iS5). A UV-vis spectrophotometer (Shimadzu UV-1800) was used for BG ($\lambda_{\text{max}} = 624$ nm) analysis. A pH meter (Eutech Instrument model pH 2700) was used for determination pH values.

Results and Discussion

Characterization of BP and JFP

BP and JFP were characterized by proximate and ultimate analyses, BET surface area, SEM, point of zero charge (pH_{zpc}), and FT-IR, and the physicochemical characteristics of both peels were obtained.

Proximate and ultimate analysis

The proximate analysis of dry BP and JFP was carried out to determine the moisture%, ash%, volatile matter%. The ultimate analysis was carried out to determine C, H, N, and S contents. The results of proximate and ultimate analyses are presented in Table 2. The presence of high volatile matter and carbon and low ash contents confirm the organic nature of adsorbents. The trace amount of sulfur in these materials makes them suitable for gasification.

BET Surface area

The BET surface area of BP and JFP is 0.65 and 1.15 m^2/g , respectively. The low surface area of these materials may be due to the operating complexity

Table 2 — Proximate and ultimate analysis of BP and JFP.

FP	Proximate analysis				Ultimate analysis			
	%Moisture	%Ash	%Volatile Matter	%Fixed Carbon	%N	%C	%H	%S
BP	9.80	5.01	85.26	0.07	1.30	40.24	6.14	0.09
JFP	6.48	6.32	86.28	0.92	0.90	40.04	5.86	0.12

associated with degassing lignocellulosic samples. Moreover, the low surface area is a characteristic feature of carbonaceous materials. Thus, it is difficult to determine the surface area of lignocellulosic wastes; the BP and JFP power is burnt before reaching the degassing temperature. The degassing temperature is thus limited to 100°C; consequently, moisture is not removed completely, and hence the low surface area^{25, 26}.

Scanning electron microscopy analysis

The surface morphology of BP and JFP is presented in Fig. 1(a and b), respectively. The surface of RBP and JFP is rough and demonstrates a heterogeneous character. Compared with BP, the surface of JFP has long flakes, which contain more micropores and macropores.

Point of zero charge

The point of zero charge of the adsorbent can be explained based on its pH_{zpc} value. The pH_{zpc} value also helps to determine the degree of ionization of functional groups present on the adsorbent surface and their possible interactions with the adsorbate molecules. The pH_{zpc} values for BP and JFP were determined according to the salt addition method (0.1N KNO_3) reported elsewhere²⁷. The pH_{zpc} of BP and JFP (Fig. 2) was found to be 4.98 and 4.16, respectively.

FT-IR analysis

FTIR study was carried out to determine the interactions between the adsorbent (BP/JFP) and adsorbate (BG). It is essential to understand the functional groups present on the surface of adsorbent. The FTIR spectral comparison between raw adsorbents and dye-loaded BP/JFP is given in Fig. 3.

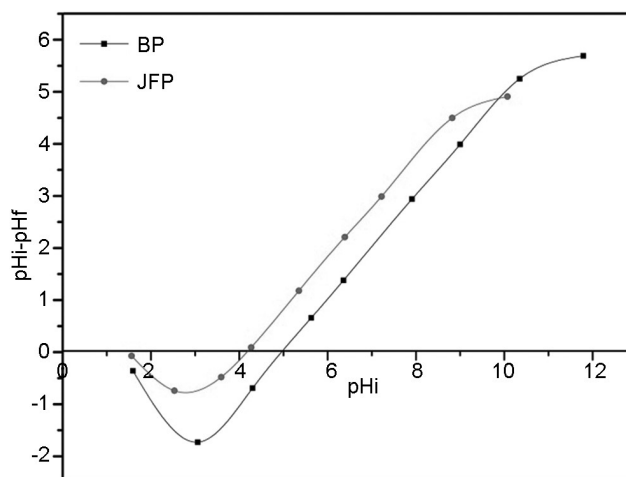


Fig. 2 — pH_{zpc} of BP and JFP

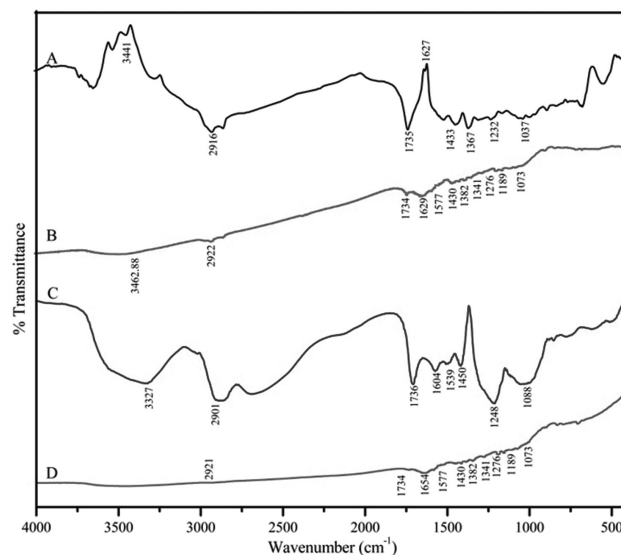


Fig. 3 — FT-IR spectra: (a) BP, (b) BG-loaded BP, (c) JFP and (d) BG-loaded JFP

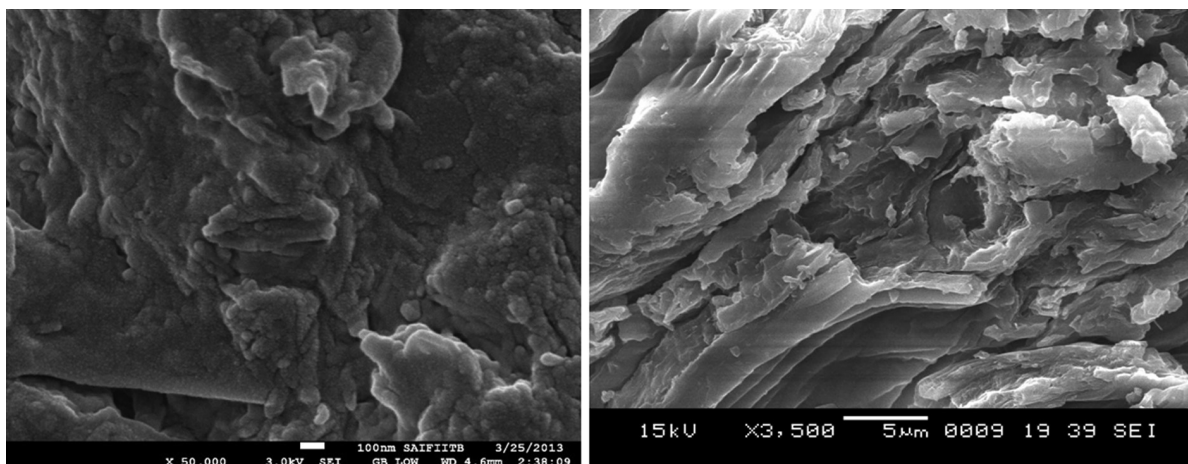


Fig. 1(a) — SEM images: (a) BP; (b) JFP

FTIR spectrum confirms the presence of alcohol, carboxylic acid, alkanes, alkyl halide, amines, amino acids, and phenol in BP and JFP.

The stretching absorption band centered at 3441.01 cm^{-1} represents the OH or NH group in BP, which is shifted to 3462 cm^{-1} after adsorption. The band observed at around 2916 cm^{-1} is assigned to stretching vibrations of $-\text{CH}_3$ or $-\text{CH}_2$ groups in carboxylic acid and its bending vibration is at around 1367 cm^{-1} , which is shifted to 2922 cm^{-1} and 1382 cm^{-1} , respectively, after adsorption. The peak at 1627 cm^{-1} is assigned to the C=C stretch of alkene, aromatic, or amino acids in BP, and this peak shifts to 1629 cm^{-1} . The carbonyl stretching band of aldehyde is observed at 1735 cm^{-1} and this is shifted to 1734 cm^{-1} . The peaks at 1232 cm^{-1} and 1037 cm^{-1} suggest the presence of phenol or tertiary alcohol; C–O stretch and primary amine also show some shifts at 1276 cm^{-1} and 1073 cm^{-1} , respectively.

In case of JFP, the strong peaks at 3327 cm^{-1} represent the OH or NH group, and the peak at 2901 cm^{-1} is attributed to the stretching vibrations of $-\text{CH}_3$ or $-\text{CH}_2$ groups in carboxylic acid; however, all these peaks disappear following BG adsorption. This may be due to the interactions of these groups with BG in the adsorption process. An intense peak observed at 1736 cm^{-1} shows the carbonyl stretching band of aldehyde, which is shifted to 1734 cm^{-1} . The peak at 1604 cm^{-1} is shifted to 1654 cm^{-1} , which is assigned to the C=C stretch of alkene, aromatic, or amino acids in JFP. The peak at 1539 cm^{-1} is shifted to 1522 cm^{-1} , which is assigned to the C=C ring stretch conjugated with C=N; the peak at 1088 cm^{-1} confirms the presence of primary amine, which is shifted to 1073 cm^{-1} .

The peaks at 1189 cm^{-1} and 1341 cm^{-1} are due to aromatic C–N stretching and C–H deformation of BG after its adsorption on BP and JFP. In addition, the new peak at 1577 cm^{-1} after adsorption shows the presence of aromatic C=C ring stretch conjugated with C=N in the quinoid structure of BG. This confirms the adsorption of BG onto BP and JFP².

Influence of operating and process parameters

The knowledge of operating and functional parameters is important in designing any adsorption system. The effects of different operational parameters (e.g., adsorbent dose, contact time, pH, and temperature) and process parameter (e.g., initial BG concentration) were studied, and our analyses are presented in the following sections.

Effect of adsorbent dosage

Adsorbent dosage is one of the main factors investigated in batch mode studies. It defines the capacity of an adsorbent for a specified initial concentration of the adsorbate.

The effect of adsorbent dosage on BG removal was studied by varying the amount of BP/JFP (0.1–0.9 g/50 mL), which was added to 50 mg/L of BG solution. This solution mixture was kept for 60 minutes in an ultrasonic bath at 30°C .

Ideally, with the increase in adsorbent dosage, the adsorption process also increases because of the initial availability of more active spots for adsorption. At one point, further increase in the adsorbent dosage does not bring any substantial change in the BG removal. This point was chosen as the optimal dosage of adsorbent (0.5g/50 mL for BP and 0.3g/50 mL for JFP). The effect of adsorbent dosage on BG removal is shown in Fig. 4a. With the increase in adsorbent dosage, the adsorption capacity was found to decrease.

Effect of contact time

Contact time studies are useful in determining the equilibrium time for the given adsorption process and for understanding the amount of dye adsorbed at different time intervals with the defined adsorbent dosage. Therefore, it becomes a very crucial factor for designing an efficient wastewater treatment system. The variation in the percentage removal of BG at different contact times for 50 mL of BG solution of different initial concentrations (20–150 mg/L) with adsorbent dosages of 0.5 g/50 mL for BP and 0.3g/50 mL for JFP is given in Fig. 4b and 4c, respectively. It can be seen from Fig. 4(b and c) that rapid adsorption occurred in the first 2 minutes of adsorption. This was followed by a steady adsorption rate until the system reaches equilibrium (~25 min). After achieving equilibrium, the adsorption of BG was negligible. Thus, we chose 25 min as the equilibration time for further adsorption studies.

It may also be observed from Fig. 4(b and c) that more than 85% of BG adsorption occurs within the first 20 min, following which it increases gradually. From the graph it is clear that about 70–80% adsorption occurs in the first 2 min, and after this period, the adsorption rate of BG becomes steady and reaches more than 98% at the equilibrium. In addition, the adsorption capacity for both the adsorbents increases with increase in time. Removal of BG is more on JFP as compared with BP.

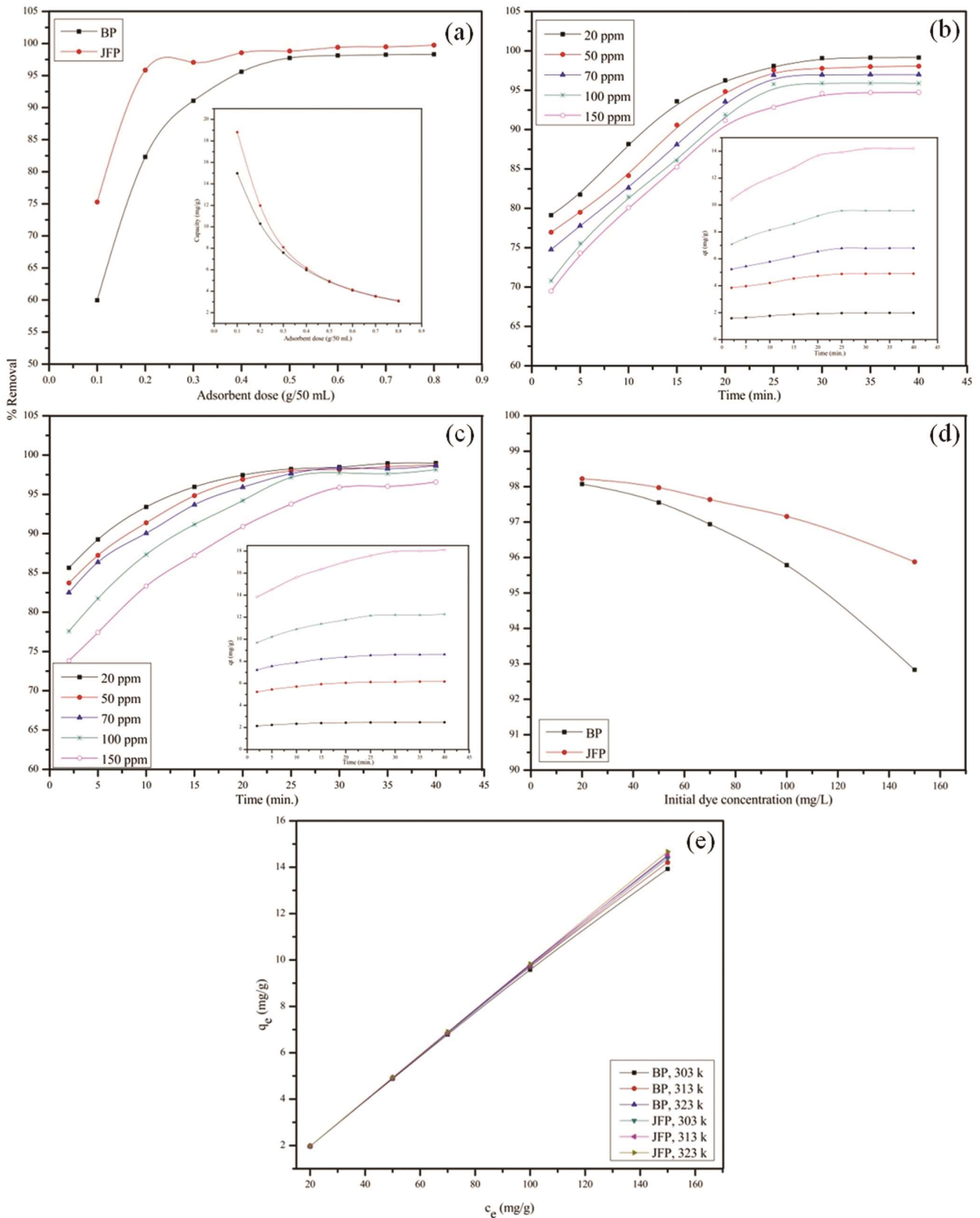


Fig. 4 — Effect of operating parameters on adsorption of BG on BP and JFP

Effect of solution pH

The stability and structure of dye molecules along with the dissociation of functional groups on the adsorbent are mainly controlled by solution pH. The pH of BG solution was found to be about 6.1 for the concentration range studied and does not change much with the dilution. At a lower pH, BG decolorizes due to the structural changes¹², whereas at higher pH values, the BG solution becomes unstable and turbid. A similar observation was also noted by many authors^{2,5,7,12}. BG is stable at natural pH, that is, at the pH_{zpc} of adsorbents⁶ (4.98 for BP and 4.16 for JFP). Thus, all the adsorption experiments were carried out without any pH adjustment.

Effect of initial concentration

The adsorption process is highly affected by the initial concentration of solution, as an initial concentration provides the necessary driving force to the dye molecule. The initial concentration of dye ranged between 20 and 150 mg/L. The maximum adsorbent dose of BP and JFP was maintained at 0.5 g/50 mL and 0.3 g/50 mL, respectively at 303K. Figure 6 shows the change in percentage removal with the change in initial concentration. For an initial concentration of 20-150 mg/L, the percentage adsorption of BG for BP and JFP reduced from 98.08 to 92.83% and from 98.23 to 95.88%, respectively. It was also found that the amount of BG adsorbed per unit mass of BP and JFP increased with increase in initial concentration (Fig. 4d).

Effect of temperature

Adsorption study was carried out at temperatures of 303, 313, and 323 K at different initial concentrations between 20 and 150 mg/L at optimal experimental conditions and natural pH of BG. Variation of adsorption capacity (q_e) with the initial concentration (c_e) is given in Fig. 4e. The adsorption capacity of BP and JFP increases with increase in temperature. This suggests the favorability of BG adsorption at higher temperature on BP and JFP.

Adsorption kinetics

Adsorption kinetics helps to determine the uptake rate of BG on BP and JFP and thus its effectiveness at different time intervals. This removal rate of BG substantially controls the diffusion process. Kinetics of adsorption can be governed by various independent mechanisms acting in parallel or in series. This mechanism includes film diffusion, chemisorption, and intraparticle diffusion¹.

Various kinetic models, for example, Lagergren first-order, pseudo-second-order, Elovich, and intraparticle diffusion^{23,27}, were applied to understand the adsorption kinetics of BG onto BP and JFP.

The equation for Lagergren-first-order kinetic model is given as

$$\ln(q_e - q_t) = \ln q_e - k_1 t \quad \dots (3)$$

The values of k_1 and q_e were determined from the graph of $\log(q_e - q_t)$ versus t .

The equation for pseudo-second-order kinetic model is given as

$$\frac{t}{q_t} = \frac{1}{k_2 q_e^2} + \frac{t}{q_e} \quad \dots (4)$$

The values of k_2 and q_e were determined from the graph of t/q_t versus t .

The equation for Elovich is given as

$$q_t = \frac{1}{\beta} \ln(\alpha\beta) + \frac{1}{\beta} \ln t \quad \dots (5)$$

The values of Elovich constants α and β are calculated from the graph of q_t versus t .

Intraparticle diffusion was used to detect the diffusion mechanism and is given by

$$q_t = k_{id} t^{1/2} + C \quad \dots (6)$$

In the Weber–Morris intraparticle diffusion model, if the graph of q_t versus $t^{0.5}$ is a straight line, then the adsorption process is predominated by intraparticle diffusion only; if multi linear plots are obtained, it can be deduced that two or more steps are involved in the adsorption process.

The kinetic parameters calculated for the pseudo-first-order, pseudo-second-order, and Elovich models are listed in Table 3. For the pseudo-first-order model, the R^2 value for BP and JFP is less than 1, which indicates that this model does not fit with our experimental data for the adsorption of BG on BP and JFP.

By contrast, for the pseudo-second-order model, the R^2 value for both adsorbents is close to 1, suggesting that the adsorption of BG follows this kinetic model. The adsorption data are also well fitted to the pseudo-second-order kinetic model, which suggests that the adsorption rate of BG is more dependent on the availability of adsorption sites rather than on the concentration of BG in the solution²⁸.

The Elovich kinetic model presents good data fit to the experimental values (Table 3), indicating that chemisorption, which occurs through ion exchange, may possibly be one of the rate-determining steps²⁹.

Table 3 — Kinetic parameters for adsorption of BG on BP and JFP

BG Concentration (mg/L)	BP			JFP		
Lagergren-first-order kinetic model						
	K_1	q_e	R^2	K_1	q_e	R_2
20	0.13	0.60	0.97	0.15	0.48	0.98
50	0.11	0.56	0.93	0.14	1.37	0.97
70	0.09	2.23	0.93	0.12	1.84	0.98
100	0.09	3.38	0.95	0.11	3.22	0.99
150	0.14	5.75	0.89	0.10	5.79	0.97
Pseudo-second-order kinetic model						
	K_2	q_e	R^2	K_2	q_e	R^2
20	0.48	2.02	0.99	0.75	2.50	0.99
50	0.16	3.92	0.99	0.24	6.25	0.99
70	0.10	7.01	0.99	0.17	8.71	0.99
100	0.07	9.92	0.99	0.08	12.44	0.99
150	0.05	14.52	0.99	0.04	18.49	0.99
Elovich model						
	A	β	R^2	A	β	R^2
20	1227.02	6.26	0.95	860241.96	7.70	0.99
50	1489.37	2.39	0.91	248659.78	2.73	0.98
70	1131.51	1.63	0.91	188328.15	1.89	0.98
100	559.12	1.03	0.92	9056.07	1.03	0.97
150	875.11	0.71	0.95	7444.22	0.69	0.96

The Weber–Morris plot (Fig. 5 a,b) is multilinear in nature, suggesting the involvement of more than one step in the adsorption of BG onto BP and JFP. The first section in the Webber–Morris plot represents the resistance to the external mass transfer surrounding the adsorbent particle, which is significant only in the early adsorption stages. The intraparticle diffusion process dominates the second portion of the Webber–Morris plot; however, even this stage is characterized by slow adsorption. The third stage represents micropore diffusion. In this stage, the rate of the intraparticle diffusion slows down. This is also called the “equilibrium stage” where maximum adsorption occurs.

From Fig. 5a and b it is clear that no line passes through the origin. This gives the nonzero values of Y intercept (C), and represents boundary-layer resistance in the early stages of adsorption. The values of C (Table 4) represent the thickness of boundary layer, and these increase for both BP and JFP with time, which confirms the increase in the thickness and effect of boundary layer on the adsorption of BG on these adsorbents. This observation suggests that intraparticle diffusion is involved in adsorption; however, this is not the single rate-controlling step. The values of all the constants for the Webber–Morris equation are given in Table 4.

Adsorption isotherm

The equilibrium isotherm plays a key role in design of adsorption system. The mode of interactions between the solute and adsorbent is also described by the adsorption isotherms. In this study, two isotherm

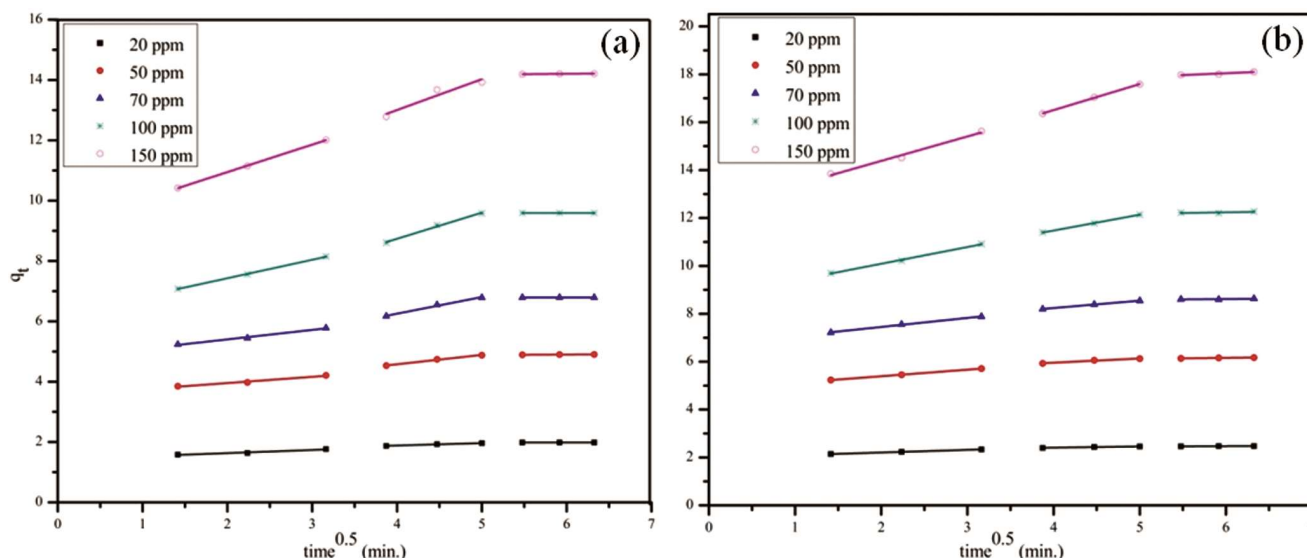


Fig. 5 — Weber–Morris plot for adsorption of BG on BP and JFP

Table 4 — Values of Webber–Morris constants

Concentration	BP			JFP		
	K _{id1}	C	R ²	K _{id1}	C	R ²
20	0.11	1.42	0.96	0.11	1.98	1
50	0.21	3.54	0.98	0.28	4.84	0.99
70	0.32	4.77	0.99	0.41	6.93	0.99
100	0.61	6.20	0.99	0.75	9.13	0.97
150	0.91	9.13	0.99	1.25	12.81	0.96
	K _{id2}	C	R ²	K _{id2}	C	R ²
20	0.08	1.57	0.99	0.05	2.21	0.98
50	0.31	3.34	0.99	0.18	5.26	0.98
70	0.55	4.05	0.99	0.68	6.36	1
100	0.87	5.27	0.99	1.46	7.44	0.99
150	1.02	8.92	0.93	2.31	10.14	0.99
	K _{id3}	C	R ²	K _{id3}	C	R ²
20	0.002	1.97	0.91	0.02	2.38	0.81
50	0.015	4.80	0.90	0.04	5.92	0.99
70	0.001	6.78	0.90	0.20	7.88	0.69
100	0.001	9.59	0.02	0.18	11.64	0.52
150	0.023	14.07	0.87	0.16	17.48	0.14

Table 5 — Adsorption isotherm parameters for adsorption of BG on BP and JFP

	T(K)	Langmuir			Freundlich			
		q _m (mg/g)	K _L (L/mg)	R ²	R _L	K _f (L/g)	n	R ²
BP	303	18.18	0.29	0.99	0.03	3.92	1.71	0.98
	313	19.49	0.33	0.99	0.03	4.50	1.61	0.97
	323	21.74	0.39	0.99	0.03	5.52	1.51	0.78
JFP	303	23.36	0.26	0.99	0.04	4.47	1.43	0.99
	313	25.97	0.26	0.99	0.04	5.06	1.37	0.99
	323	31.25	0.27	0.99	0.04	6.21	1.28	0.99

models, namely, Langmuir and Freundlich³⁰, were used to define the equilibrium adsorption of BG onto BP and JFP.

The Langmuir isotherm model assumes mono layer adsorption on the adsorbent surface having a fixed number of definite localized sites with no lateral interactions or steric hindrance between the adsorbed molecules and the adjacent sites. The linearized Langmuir adsorption model can be given as

$$\frac{C_e}{q_e} = \frac{C_e}{q_m} + \frac{1}{q_m K_L} \quad \dots (7)$$

The constants (q_m and K_L) for Langmuir isotherms can be calculated from the graph of C_e/q_e versus C_e, which gives a straight line with slope 1/q_m and intercept 1/(q_mK_L).

The dimensionless constant, commonly known as “separation factor” (R_L) can be represented as

$$R_L = \frac{1}{1 + C_e K_L} \quad \dots (8)$$

The value of R_L explains the isotherm type to be either favorable (0 < R_L < 1), irreversible (R_L = 0),

linear (R_L = 1), or unfavorable (R_L > 1). Lower R_L indicates the more favorability of adsorption.

The Freundlich adsorption isotherm generally indicates multilayer adsorption along with the uneven distribution of heat and affinities for adsorption above the heterogeneous surface. The Freundlich isotherm model can be represented as follows:

$$\log q_e = \log k_f + \frac{1}{n} \log C_e \quad \dots (9)$$

The Freundlich adsorption constants, K_F and n, can be calculated by the linear plot of log q_e versus log C_e.

The Freundlich constant n signifies the favorability of the adsorption process. If the slope (1/n) is between 0 and 1, the intensity of adsorption is more or the adsorbent surface is heterogeneous. In addition, if this value is close to zero, it indicates the increased heterogeneity of adsorbent surface. The Freundlich adsorption capacity of the adsorbent is explained by K_F [mg/g (L/mg)^{1/n}].

The calculated parameters for the Langmuir and Freundlich adsorption isotherms are presented in Table 5. The results show that the Langmuir isotherm

best fit the adsorption of BG onto BP, whereas both Langmuir and Freundlich isotherm show better fit for the BG adsorption onto JFP. This suggests that the adsorption of BG onto JFP is multilayer in nature. As a result, the adsorption capacity of JFP is more than that of BP for BG uptake. The values of R_L confirm that both BP and JFP are favorable for adsorption of BG under considered conditions. The Langmuir adsorption capacity for BG removal on BP was 21.739 mg/g, whereas on JFP it was 31.250 mg/g. The values of $1/n$ lie in the range of 0 and 1, indicating favorable adsorption at all temperatures.

Adsorption Thermodynamics

The effect of temperature on the adsorption of BG onto BP and JFP was studied in the temperature range of 303–323 K at optimized conditions.

The Gibbs free energy change is related to the heat of adsorption and entropy change at constant temperature (equation 10)²⁷.

$$\Delta G = \Delta H + T\Delta S \quad \dots (10)$$

The Gibbs free energy change of the adsorption process is also associated with the equilibrium constant explained by the classical van't Hoff equation as given in equation 11.

$$\Delta G = -RT \ln K_d \quad \dots (11)$$

Relating equations 10 and 11, we get

$$\ln K_d = \frac{\Delta S}{R} - \frac{\Delta H}{RT} \quad \dots (12)$$

The values of ΔH and ΔS can be calculated from the slope and intercept of van't Hoff plot ($\ln K_d$ vs. $1/T$)³¹.

The ΔH value provides information about the strength of bonding between BG and adsorbents studied (BP and JFP). Table 6 presents the thermodynamic parameters for BG adsorption onto BP and JFP. The positive value of ΔS indicates the increased randomness at the solid–solution interface and augmentation in the degree of freedom of BG. The positive values of ΔH confirm the endothermic nature of adsorption.

The ΔG value of adsorption of BG onto BP and JFP is negative, which is as expected for a spontaneous process. The decrease in values of ΔG with increase in temperature indicates that higher temperatures are suitable for the adsorption process. At higher temperatures, the adsorbent surface is activated and/or there is enlargement of pores on the adsorbent surface. This might be the possible reason for higher adsorption capacity at high temperatures.

After adsorption loaded with cationic dyes need not be regenerated and can be disposed by direct burning¹. As BG is cationic in nature and both the adsorbents (BP/JFP) are biodegradable. The used adsorbent can be further utilized for generation of power (by gasification). The proposed method is to avoid any downstream processing, but instead value-added products like syngas and bio-char makes the process eco-friendly and economical³².

Adsorption of BG on other adsorbents prepared from agricultural waste was compared with BP and JFP and the results are presented in Table 7. The adsorption capacity for BG removal on BP and JFP is higher than other reported natural adsorbents; however, the adsorption capacity of the studied adsorbents (BP and JFP) is less than that of the chemically modified adsorbents. Besides, BP and JFP are cheap and easily available, and therefore, their use for the removal of BG is economically advantageous.

Table 6 — Thermodynamic parameters for adsorption of BG on BP and JFP

	C_0 (mg/L)	ΔH (KJ/mol)	ΔS (J/mol K)	ΔG (KJ/mol)		
				303 K	313 K	323 K
BP	20	254.50	40.99	-9902.82	-10686.65	-11691.31
	50	298.39	40.36	-9283.85	-10107.01	-11230.77
	70	353.55	40.32	-8705.84	-9684.65	-10846.38
	100	443.79	40.54	-7868.88	-9033.81	-10346.89
	150	455.89	36.18	-6452.31	-7500.41	-8907.99
JFP	20	216.08	40.45	-10111.05	-10872.55	-11734.48
	50	266.30	39.58	-9768.86	-10431.35	-11437.74
	70	263.14	39.48	-9374.92	-10107.40	-11176.40
	100	203.60	39.37	-8898.60	-9741.48	-10853.38
	150	392.43	38.96	-7927.11	-8888.70	-10201.16

Table 7— Comparison of maximum adsorption capacities of BG on different adsorbents

Adsorbent	Presence of Ultrasonic field	Capacity (mg/g)	Reference
<i>Psidiumguajavaleaves</i>	No	1.07	4
<i>Solanumtuberosum</i> peel	No	1.17	4
Oxidized cactus fruit peel	No	166.66	6
Activated carbon prepared from acorn	No	2.11	11
Watermelon rind	No	92.60	12
Acid-activated watermelon rind	No	188.60	12
Spent tea leaves	No	9.57	13
Jackfruit peel	No	9.47	13
Rambutan peel	No	9.64	13
Mangosteen peel	No	9.27	13
RHA-MCM-41	No	250.00	2
Poly(acrylic acid) hydrogel composite	No	26.31	3
Surfactant Doped Polyaniline/MWCNTs Composite	No	476.19	7
BP	Yes	21.74	This study
JFP	Yes	31.25	This study

Conclusion

The results of this study show that BP/JFP can be used as an adsorbent for the removal of MB dye from aqueous solutions. The amount of MB dye adsorbed is influenced by adsorbent dose, contact time, initial dye concentration, and temperature. Both the amount of BG adsorbed and the rate of adsorption increased in the presence of ultrasonic field. The adsorption of BG onto BP and JFP reached equilibrium within 25 min. The adsorption process follows pseudo-second-order kinetic model, which suggests that the adsorption rate of BG is more dependent on the adsorption sites available rather than on the concentration of BG in the solution. The Langmuir isotherm shows the best fit for the adsorption of BG onto BP, whereas both Langmuir and Freundlich adsorption isotherms show best fit for the adsorption of BG onto JFP. The maximum adsorption capacities calculated using the Langmuir isotherm were 21.739 mg/g and 31.250 mg/g at 313 K for BP and JFP, respectively. The ΔG values were negative at all operating temperatures, confirming that the adsorption of BG was spontaneous and thermodynamically favorable. The positive value of ΔS suggests the increased randomness at the adsorbate-adsorbent interface. Overall, our study results suggest that BP and JFP can be used as an ecofriendly and low-cost agro material for removal of BG dye from aqueous solutions.

References

- 1 Pathak P D, Mandavgane S A & Kulkarni B D, *Rev Chem Eng*, 31 (2015) 361.
- 2 Dutta R, Nagarjuna T V, Mandavgane S A & Ekhe J D, *Ind Eng Chem Res*, (2014) 18558.
- 3 Shirsath S R, Patil A P, Patil R, Naik J B, Gogate P R & Sonawane S H, *Ultrasonics Sonochem* 20 (2013) 914.
- 4 Rehman R, T Mahmud & M Irum, *J Chem*, (2015) 1.
- 5 Bhattacharyya K G & Sarma A, *Dyes and Pigments*, 57 (2003) 211.
- 6 Kumara R & Barakat M A, *Chem Eng J*, 226 (2013) 377.
- 7 Kumar R, Ansari M O & Barakat M A, *Ind Eng Chem Res*, 53 (2014) 7167.
- 8 Anastopoulos I & Kyzas G Z, *J Mol Liq* 200 (2014) 381.
- 9 Salleh M A M, Mahmoud D K, Karim W A W A & Idris A, *Desalination* 280 (2011) 1.
- 10 Yagub M T, Sen T K, Afroze S & Ang H M, *Adv Colloid Interface Sci*, 209 (2014) 172.
- 11 Ghaedi M, Soylak M, Purkait M K, Hossainian H, Montazerzohori M, Shokrollahi A & Shojai pour F, *Desalination*, 281 (2011) 226.
- 12 Lakshmi pathy R, Reddy N A & Sarada N C, *Desalination and Water Treatment*, (2014), 1.
- 13 Nora N M, Hadibaratab T, Yusopa Z & Lazim Z M, *J Technol (Scie & Eng)*, 74(2015)117.
- 14 Hamdaouia O & Naffrechoux E, *Ultrasonics Sonochem*, 16 (2009)15.
- 15 Breitbach M & Bathen D, *Ultrasonics Sonochem*, 8 (2011)277.
- 16 Midathana V R & Moholkar V S, *Ind Eng Chem Res*, 48 (2009)7368.
- 17 Roosta M, Ghaedi M, Shokri N, Daneshfar A, Sahraei R & Asghari A, *Spectrochimica Acta Part A*, 118 (2014) 55.
- 18 Roosta M, Ghaedi M, A Daneshfar, Sahraei R & Asghari A, *Ultrasonics Sonochem*, 21(1) (2013) 242.
- 19 Jing G, Zhou Z, Song L & Dong M, *Desalination*, 279 (2011)423.
- 20 Eren Z, *J Environ Manag*, 04 (2012)127.
- 21 Hamdaouia O, Chiha M & Naffrechoux E, *Ultrasonics Sonochem*, 15 (2008) 799.
- 22 Djelloul C & Housseine A, *Desalination and Water Treatment*, 51 (2013)5805.
- 23 Pathak P D, Mandavgane S A & Kulkarni B D, *Desalination and Water Treatment*, (2015), 1.

- 24 Indian standard Standard, Fourth Reprint july 2006.
- 25 Sharma A & Bhattacharyya K G, *Ind J Chem Tech*, 12(2005) 285.
- 26 Castro R S D, Caetano L, Ferreira G, Padilha P M, Saeki M J, Zara L F, Martines M A U & Castro G R, *Ind Eng Chem Res*, 50(2011) 3446.
- 27 Pathak P D & Mandavgane S A, *J Environ Chem Eng*, 3(2015) 2435.
- 28 Njokua V O & Hameed B H, *Chem Eng J*, 173(2011) 391.
- 29 Khaskheli M I, Memon S Q, Siyal A N & Khuhawar M Y, *Waste and Biomass Valor*, 2(2011) 423.
- 30 Foo K Y & Hameed B H, *Chem Eng J*, 156(2010) 2.
- 31 Liu R-L, Liu Y, Zhou X-Y, Zhang Z-Q, Zhang J & Dang F-Q, *Bioresource Tech*, 154 (2014) 138.
- 32 Pathak P D, Mandavgane S A & Kulkarni B D, *Desalination and Water Treatment*, 57 (2015) 1.